論文内容の要旨

論文題目　Interfacial Synthesis of Coordination Nanosheets Comprising Terpyridine and Dithiolato Ligands and Exploration of Their Functionalities

（テルピリジンおよびジチオラト配位子を用いた配位ナノシートの界面合成と
その機能性の探求）

氏　名　髙田　健司

1. Introduction

Since the discovery of graphene, many scientists have devoted their efforts to the research on two-dimensional nanomaterials, nanosheets. Recently nanosheets woven up by coordination bonds have appeared as a new family of nanosheets. While graphene and other inorganic nanosheets such as metal chalcogenides are obtained by the exfoliation of their bulk layered materials, coordination nanosheets are synthesized by bottom-up methods using coordination bonds. The tunability of ligands and metal ions ensures a wide variety of functionality in metal complex nanosheets. However, most of reports of coordination nanosheets have focused on the preparation of them. The aim of this study is the realization of functional coordination nanosheets comprising a tpy (tpy = 2,2':6',2"-terpyridine) ligands and porphyrazine-conjugated dithiolato ligand, and the evaluation of electrochemical or photochemical properties of these nanosheets.

2. Electrochromic bis(terpyridine)metal complex nanosheets

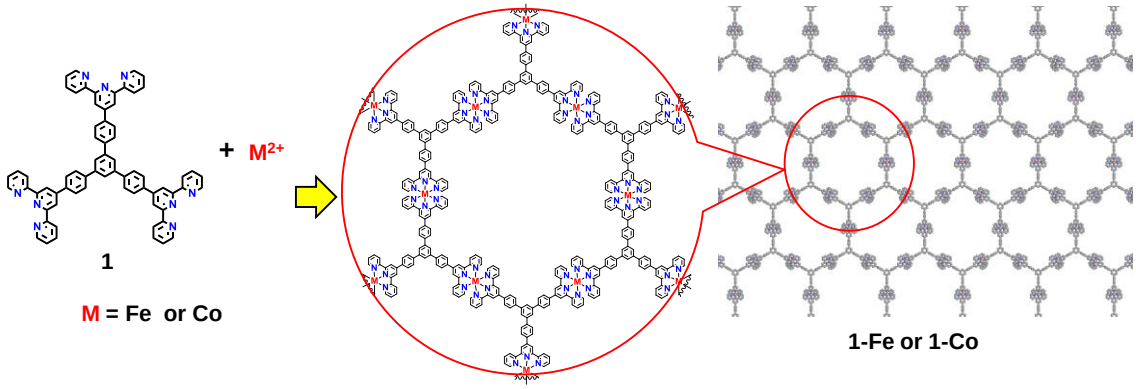

Figure 1. Chemical structure of ligand **1** and bis(terpyridine) complex nanosheets **1-Fe** and **1-Co**.

2.2 Bis(terpyridine)iron(II) complex nanosheet

Bis(terpyridine)iron(II) complex nanosheet **1-Fe** (Figure 1) was designed and prepared for the redox activity of $[Fe(tpy)_2]^{2+}$. To synthesize the desired nanosheet, a liquid-liquid interfacial coordination reaction between a dichloromethane solution of **1** and an aqueous solution of $Fe(BF_4)_2$ was employed. Undisturbed standing of the double layered system for 1 day led the generation of **1-Fe** at the interface as a purple film. Transmission

electron microscopy (TEM) and scanning electron microscopy (SEM) images of the film showed that **1-Fe** had a flat layered structure. Atomic force microscopy (AFM) also revealed the morphology of **1-Fe**. From its cross-sectional analysis, the thickness of **1-Fe** was ca. 200 nm. Peak positions and peak intensities in X-ray photoelectron spectroscopy (XPS) supported that **1-Fe** was composed of $[Fe(tpy)_2]^{2+}$ units. These series of data identified **1-Fe** as the designed bis(terpyridine)iron(II) complex nanosheet.

The cyclic voltammogram of **1-Fe** immobilized on an ITO electrode exhibited one reversible oxidation wave at 0.68 V *vs.* Fc^+/Fc (Fc = ferrocene), which was attributable for the $[Fe(tpy)_2]^{3+}/[Fe(tpy)_2]^{2+}$ redox couple. This redox reaction accompanied the color change of **1-Fe**, so-called electrochromism. Upon the oxidation, **1-Fe** was bleached into pale yellow, and the re-reduction reproduced the original color of the nanosheet. In UV-vis spectroscopy, the MLCT absorption band at λ_{max} = 578 nm completely diminished after the oxidation, and the re-reduction induced the revival of the peak (Figure 2a). The repetitive potential-step chronoamperometry (PSCA) measurements ensured the high durability of **1-Fe** against more than 800 redox cycles and fast color change within 0.35 s (Figure 2b).

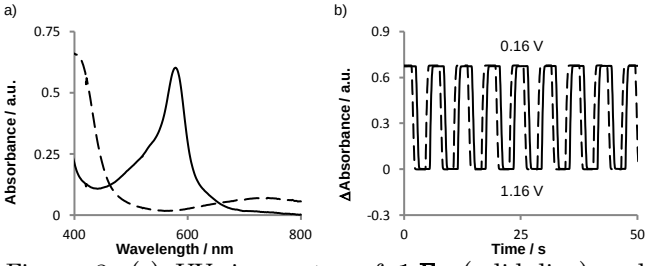

Figure 2. (a) UV-vis spectra of **1-Fe** (solid line) and oxidized **1-Fe** (dotted line). (b) Absorptivity under PSCA measurement (solid line; 1st cycle ~, dotted line; 801st cycle ~)

2.2 Exchange of terpyridine linker

For bis(terpyridine) complex nanosheets, another terpyridine ligand with ethynylene linker was employed. The corresponding nanosheet, **2-Fe**, was prepared and identified as well as **1-Fe**. **2-Fe** also demonstrated electrochromism with quick response and high durability. **2-Fe** had a bluish color by the electron withdrawing ability of ethynylene linkers, and oxidized **2-Fe** also became slightly pale color compared to oxidized **1-Fe**. The results indicated that the modulation of electronic states in terpyridine ligands enables the fine tuning of the color in electrochromism without the degradation of electrochromic properties.

2.3 Bis(terpyridine)cobalt(II) complex nanosheet

Bis(terpyridine)cobalt(II) complex nanosheet **1-Co** was designed for the multi-colorization of the electrochromic nanosheet system. The preparation of **1-Co** was conducted by the same interfacial coordination reaction and characterization also was accomplished by the same methods.

Cyclic voltammetry of **1-Co** physically adsorbed on an ITO electrode showed a redox wave at -1.15 V *vs.* Fc^+/Fc, which was assignable to the $[Co(tpy)_2]^{2+}/[Co(tpy)_2]^{+}$ redox couple. This redox process also accompanied electrochromism; The reduction of $[Co(tpy)_2]^{2+}$ moieties colorized **1-Co** in purple. UV-vis spectrum of reduced **1-Co** presented a broad absorption band around 600 nm (Figure 3)

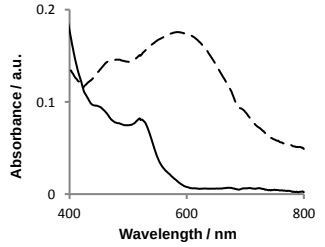

Figure 3. UV-vis spectra of **1-Co** (solid line) and reduced **1-Co** (dotted line).

2.4 Fabrication of solidified electrochromic device

Electrochromic behaviors of bis(terpyridine) metal complex nanosheets mentioned above were measured in a solution media. The application for electrochromic devices such as displays requires the solidification of the system. Therefore, solidified electrochromic devices with **1-Fe** and **1-Co** were fabricated by employing Bu_4NClO_4-containing polyvinylchloride (TBAP@PVC) as a supporting electrolyte. This electrolyte containing polymer was sandwiched by two ITO electrodes. One of the electrodes was modified with nanosheet, which was regarded as a working electrode here. Both devices with **1-Fe** and **1-Co** showed reversible color change with the applied voltages of +3.0 V and -1.8 V for the **1-Fe** device and -4.5 V and 0 V for the **1-Co** device respectively.

Then, the hybridization of both nanosheets in the same device was investigated. The device structure is shown in Figure 4a. TBAP@PVC was sandwiched by two ITO electrodes. One of them was immobilized with **1-Fe**, and the other was modified with **1-Co**. Each nanosheet was shaved into the letters "U" and "T" respectively. The electrode with **1-Fe** was regarded as a working electrode. In this device, electrochemical reactions on both electrodes were identified so that unidentified or unexpected reactions on the counter electrode were avoided. The application of +2.0 V to the device resulted in the color changes of **1-Fe** and **1-Co** at the same time. When the external voltage was reduced to +1.0 V, the re-reduction of oxidized **1-Fe** and re-oxidation of reduced **1-Co** occurred. These changes in applied voltages caused the alternate display of the letters "U" and "T" (Figure 4b), realizing "dual" electrochromism.

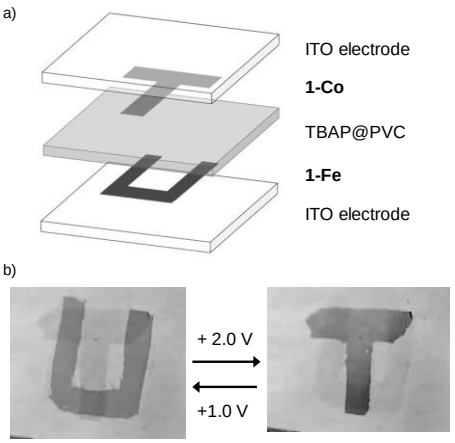

Figure 4. (a) Electrochromic device with both **1-Fe** and **1-Co**. (b) Operation of the "dual" electrochromic device.

3. Redox-active bis(terpyridine)nickel(II) complex nanosheet

The bis(terpyridine) complex system was expanded to the nickel(II) complex system. Corresponding coordination nanosheets **1-Ni** was synthesized and identified as well as other bis(terpyridine)metal complex nanosheets. **1-Ni** exhibits one chemically reversible oxidation wave at 1.21 V *vs.* Fc^+/Fc without apparent color change. The absorption changed only in the UV and near UV regions below 450 nm. This feature enables the application of **1-Ni** for charge compensating material in dual electrochromic devices, which emphasize electrochromism on another electrode.

4. Fluorescent $[Zn_2(\mu\text{-}O_2SO_2)_2(tpy)_2]$ complex nanosheet

For a metal complex nanosheet with photo-functions, Zn^{2+} and SO_4^{2-} were chosen as a metal ion and a counter anion respectively. It was reported that the coordination reaction between tpy ligands and $ZnSO_4$ gives not mononuclear $[Zn(tpy)_2]^{2+}$ but dinuclear $[Zn_2(\mu\text{-}O_2SO_2)_2(tpy)_2]$ structure (Figure 5a). A liquid-liquid

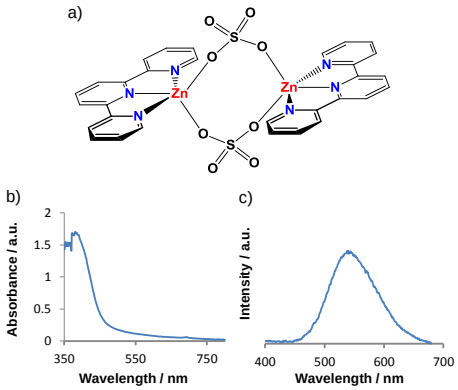

Figure 5. (a) Coordination motif of $[Zn_2(\mu\text{-}O_2SO_2)_2(tpy)_2]$. (b,c) UV-vis and fluorescence spectra of **1-Zn** on a quartz substrate.

interfacial coordination reaction between a dichloromethane solution of **1** and an aqueous solution of $ZnSO_4$ afforded **1-Zn** as a yellow film at the interface. TEM unveiled the sheet-like structure of **1-Zn**. The peak and intensity in XPS suggested that the ratio of atomic concentration in **1-Zn** was approximately 3:1 for N:Zn. Splitting of S-O stretching peaks in the infrared spectrum was attributed to breaking of symmetry around SO_4^{2-} upon the coordination to zinc ions. These results definitely indicated that coordination structure in **1-Zn** was the dinuclear $[Zn_2(\mu\text{-}O_2SO_2)_2(tpy)_2]$.

1-Zn showed fluorescence in solid state. UV-vis spectrum of **1-Zn** on a quartz substrate (Figure 5b) demonstrated the absorption in the UV region (< 400 nm). The fluorescence spectrum recorded with a 350 nm light excitation featured an emission peak at 552 nm (Figure 5c), corresponding to the fact that **1-Zn** emitted yellow light. The luminescent quantum efficiency was ca. 4 %. The emission showed solvatochromic with blue shift of the mission maximum by ca. 25 nm in acetone or ethanol.

5. Porphyrazine-hybridized nickeladithiolene nanosheet

Metallaadithiolene nanosheets have attracted considerable attentions because of their structural similarities to graphene. The previous studies developed metalladithiolene nanosheet using benzenehexathiol and triphenylenehexathiol ligands. The usage of functional backbones can endow the nanosheets to novel functions. Here, construction of nickeladithiolene nanosheet with a porphyrazineoctathiol (**3**) backbone was challenged (Figure 6).

The slow diffusion of sodium salt of **3** into a methanol solution containing Ni^{2+} afforded the black precipitate. SEM image implies the layered sheet morphology of **3-Ni**. The ultrasonication exfoliated the stacked nanosheet into a few layers confirmed by TEM. XPS and IR spectroscopy identified **3-Ni** and gave the insights into the oxidation states of nickeladithiolene moietiyes.

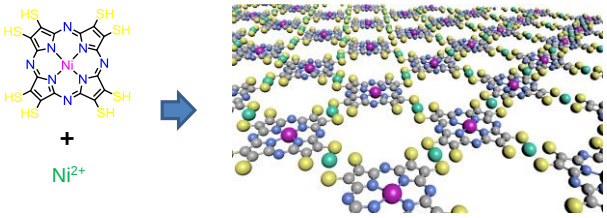

Figure 6. Nickelladithiolene complex nanosheet with porphyrazineoctathiole **3** ligand.

6. Conclusions

In summary, I have achieved the synthesis of a series of coordination nanosheets using terpyridine ligands and dithiolato ligand. I have also explored their electrochemical and photochemical functionalities. Bis(terpyridine)metal complex nanosheets showed electrochromism with rapid and repeatable response, and zinc complex nanosheets exhibited the light emission properties. For the electrochromic nanosheets, the fabrication of electrochromic devices with them were established, and the devices were successfully operated by the external voltage. These studies promise the integration of coordination nanosheets into future electronic and optoelectronic applications.